METALLURGY AND FOUNDRY ENGINEERING – Vol. 31, 2005, No. 1

Edward Fraś*, Marcin Górny**, Hugo F. López***

SOLIDIFICATION CONDITIONS OF GRAY AND WHITE CAST IRON. PART I – THEORETICAL BACKGROUND

SYMBOLS

Symbol	Meaning	Definition	Units
a	Moulding material ability to absorb heat	$a = \sqrt{k_m c_m}$	J/(cm^2·ºC·s$^{1/2}$)
A, A_1	Parameters	Eqs. (17), (25)	s$^{1/2}$/m
b	Nucleation coefficient of eutectic cells	Eq. (51)	^{o}C
B, B_1	Temperature parameters	Eqs. (20), (29)	–
c	Specific heat of metal	–	J/(cm^3·ºC)
c_{ef}	Effective specific heat of metal	Eq. (21)	J/(cm^3·ºC)
c_m	Specific heat of moulding material	–	J/(cm^3·ºC)
C_e	Carbon content in graphite eutectic	Eq. (72)	wt. %
C_γ	Carbon content in austenite	Eq. (73)	wt. %
CT	Chilling tendency	Eqs. (61), (62)	s$^{1/2}$/^{o}C$^{1/3}$
d_{cr}	Critical thickness of pins	Eq. (63)	cm
dV_m/dt	Volumetric solidification rate of an eutectic cell at maximum undercooling	Eq. (38)	cm^3/s
f_c	Real volume fraction of cementite eutectic	Eqs. (6), (10)	–
f_{ce}	Extended volume fraction of cementite eutectic	Eq. (8)	–

* M.Sc., **Ph.D., Faculty of Foundry Engineering, AGH University of Science and Technology, Reymonta 23, 30-059 Kraków, Poland; edfras@agh.edu.pl; ** Author is an award holder of the NATO Science Fellowship Programme, mgorny@agh.edu.pl

*** Prof., Department of Materials Engineering, University of Wisconsin-Milwaukee, P.O. Box 784, Milwaukee, WI 53201, USA; hlopez@uwm.edu

f_g	Real volume fraction of graphite eutectic	Eq. (5),(9)	–
f_γ	Austenite volume fraction	Eq. (70)	–
F_c	Surface area of the casting	–	cm^2
g_γ	Mass fraction of austenite	Eq. (71)	–
k_m	Heat conductivity of the mould material	–	J/(s·cm·ºC)
l	Size of substrates for nucleation of graphite	–	cm
$\langle l \rangle$	Mean size of sites (substrates) for nucleation of graphite	–	cm
L_γ	Latent heat of austenite	Table 1	J/cm^3
L_e	Latent heat of graphite eutectic	Table 1	J/cm^3
M	Casting modulus	Eqs. (47),(52)	cm
M_{cr}	Critical casting modulus	Eq.(60)	cm
n	Wedge size coefficient	–	–
N_g	Volumetric density of graphite eutectic cells	Eq. (50)	cm^{-3}
N_c	Volumetric density of cementite eutectic grain	–	cm^{-3}
N_s	Density of substrates for nucleation of eutectic cells	–	cm^{-3}
p	Cooling coefficient	Eq. (48)	$(cm\cdot{}^oC^{1/3})/s^{1/3}$
q_a	Accumulated heat flux in casting	Eq. (14)	J/s
q_m	Heat flux extracted from casting into mould casting	Eq. (13)	J/s
q_s	Heat flux generated during solidification	Eq. (15)	J/s
$Q = dT/dt$	Metal cooling rate	Eq. (27)	ºC/s
R_g	Graphite eutectic cell radius	–	cm
R_c	Cementite eutectic cell radius	–	cm
R_m	Graphite eutectic cell radius at maximum undercooling	Eq. (41)	cm
s_{cr}	Critical thickness of plates	Eq. (64)	cm
t	Time	–	s
t_l	Time at the onset of austenite solidification	–	s
t_m	Time at the maximum undercooling	Eq. (36)	s
t_s	Time at the onset of graphite eutectic solidification	–	s
T	Temperature	–	ºC
T_c	Temperature of the formation of cementite eutectic	Table 1	ºC
T_i	Initial temperature of metal in mould cavity	–	ºC
T_l	Liquidus temperature at the onset of austenite solidification	Table 1	ºC
$T_{l\gamma}$	Liquidus temperature of austenite when melt composition is equal to the maximum content of carbon in austenite	Table 1	ºC

T_m	Temperature at maximum undercooling of graphite eutectic	–	ºC
T_{mst}	Metastable equilibrium temperature for the cementite eutectic crystallization	–	ºC
T_s	Stable equilibrium temperature of the graphite eutectic crystallization	Table 1	ºC
T_w	Formation temperature only of cementite eutectic	–	ºC
u_c	Growth rate of cementite eutectic	Eq. (2)	cm/s
u_g	Growth rate of graphite eutectic	Eq. (1)	cm/s
V	Volume of eutectic cells	–	cm^3
V_c	Volume of casting	–	cm^3
V_m	Volume of a graphite eutectic cell at maximum undercooling	$(4\pi R_m^3)/3$	cm^3
w	Wedge value	Eqs. (66), (67)	cm
α_d	Thermal diffusivity of mould material	k_m/c_m	cm^2/s
β	Wedge angle	–	o
ϕ	Heat coefficient of metal	Eq. (28)	$J/(cm^3 \cdot ºC)$
μ_c	Growth coefficient of cementite eutectic	–	$cm/(s \cdot ºC^2)$
μ_g	Growth coefficient of graphite euetctic	Table 1	$cm/(s \cdot ºC^2)$
ρ_m	Density of melt	Table 1	g/cm^3
ρ_γ	Density of austenite	Table 1	g/cm^3
σ	Interfacial energy between the nucleus and melt	–	J/cm^2
θ	Wetting angle between substrate and nuclei of graphite	–	o
ΔH	Enthalpy of solidification	–	J/cm^3
ΔT_c	Undercooling degree of cementite eutectic	Eq. (4)	ºC
ΔT_g	Undercooling degree of graphite eutectic	Eq. (3)	ºC
ΔT_{sc}	Temperature range between T_s and T_c	Eq. (69)	ºC
ΔT_m	Maximum undercooling of graphite eutectic	Eq. (53)	ºC
ω	Frequency	Eq. (32)	1/s

1. INTRODUCTION

The transition from gray to white cast iron arises from the nucleation and growth competition between the stable graphite (gray) and metastable cementite (white) eutectics. In the literature [1–6] the transition from graphite to cementite eutectic during solidification is also related to the so called chill of cast iron. Chill testing of cast iron is commonly measured using the ASTM Designation A 367-55T (see Fig. 1b and Fig. 7).

By these means it is possible to identify three regions in a chill specimen (see Fig. 1b):

1) gray (graphite eutectic),
2) mottled (mixed structure of graphite),
3) cementite eutectic) and white (cementite eutectic).

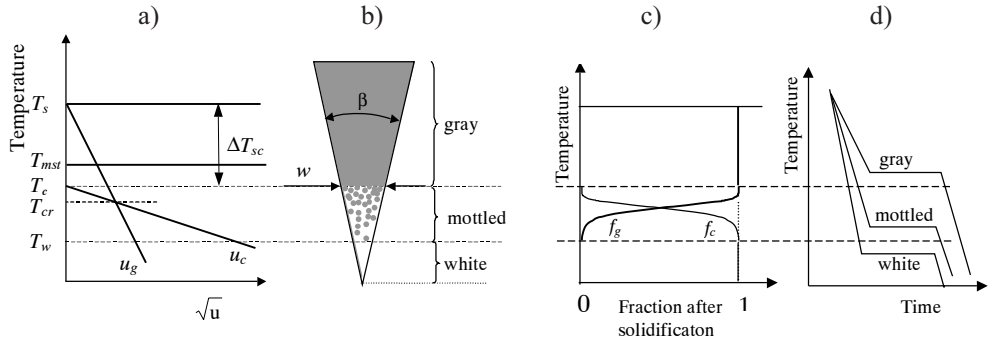

Fig. 1. *Structural transitions in cast iron: a) temperature as a function of growth rate for graphite u_g and cementite u_c eutectics; b) structure of cast iron in wedge shaped castings; c) fraction of graphite f_g and cementite f_c eutectics; d) schematic representation of the cooling curves for the solidification of gray ($T_c \le T \le T_s$), mottled ($T_w \le T \le T_c$), and white ($T \le T_w$) cast iron*

The regions containing motled or white structures are also known as the chill for castings. In general, the greater is the susceptibility for the transition from gray to white cast iron during solidification, the greater is the chill developed in cast iron.

It is well known [1–6] that the chilling tendency (CT) of cast iron determines their subsequent performance in diverse applications. In particular, cast irons possessing a high CT tend to develop zones of white or mottled iron. Considering that these regions can be extremely hard, their machinability can be severely impaired. Alternatively, if white iron is the desired structure a relatively small CT will favour the formation of gray iron. This in turn leads to low hardness and poor wear properties in the as-cast components. Hence, considerable efforts have been made in correlating the inoculation practice, iron composition, pouring temperature, etc. with the CT of cast iron [1–6].

Thus far, the mechanisms responsible for the chilling tendency of cast iron have not been clearly disclosed, with only a few attempts aimed at elucidating these mechanisms

[5–8]. In addition, various numerical models have been proposed [9–11] to predict whether a given casting or part of it will solidify according to the stable or metastable Fe-C system. However, their application is tedious due to extensive numerical calculations. Accordingly, in this work a simple analytical model is proposed to explain the mechanism responsible for the chilling tendency of cast iron containing pro-eutectic austenite. The proposed model does not take into account the segregation of alloying elements and in consequence the development of so called inverse chill.

The growth rates for graphite eutectic u_g and cementite eutectic u_c can be related to the degrees of undercooling through Eqs. (1) and (2) according to theoretical treatments on eutectic growth [12–14]:

$$u_g = \mu_g \ \Delta T_g^2 \tag{1}$$

$$u_c = \mu_c \ \Delta T_c^2 \tag{2}$$

where:

$$\Delta T_g = T_s - T \tag{3}$$

$$\Delta T_c = T_{mst} - T \tag{4}$$

in Eqs. (1) trough (4) ΔT_g is the undercooling for graphite eutectic and ΔT_c is the undercooling for cementite eutectic, and μ_g and μ_c are their respective growth coefficients, T_s, T_{mst} are the stable and metastable equilibrium temperatures of the graphite and cementite eutectics, respectively.

It is widely accepted [8, 13, 15] that the nucleation of cementite eutectic is rather difficult requiring a certain degree of undercooling to temperatures $T_c < T_{mst}$ (see Fig. 1). Below T_c both graphite and cementite eutectic grow simultaneously interfering with each other in giving rise to the final structure. From the works of Kolmogorov [16] and Kasuya [17], which take into account the impingement of eutectic cells, the real volume fractions of graphite f_g and cementite f_c eutectics can be described by:

$$f_g = \frac{f_{ge}}{f_{ge} + f_{ce}} \left\{ 1 - \exp\left[-\left(f_{ge} + f_{ce} \right) \right] \right\} \tag{5}$$

$$f_c = \frac{f_{ce}}{f_{ge} + f_{ce}} \left\{ 1 - \exp\left[-\left(f_{ge} + f_{ce} \right) \right] \right\} \tag{6}$$

where: f_{ge}, f_{ce} are the extended volume fractions of graphite and cementite eutectics, which in turn can be given by:

$$f_{ge} = \frac{4}{3}\pi N_g R_g{}^3 = \frac{4}{3}\pi N_g \left(u_g t\right)^3 = \frac{4}{3}\pi N_g \left[\mu_g \left(T_s - T\right)^2 t\right]^3 \tag{7}$$

$$f_{ce} = \frac{4}{3}\pi N_c R_c^3 = \frac{4}{3}\pi N_c \left(u_c t\right)^3 = \frac{4}{3}\pi N_c \left[\mu_c \left(T_{mst} - T\right)^2 t\right]^3 \tag{8}$$

Equations (7) and (8) assume spherical geometry, where R_g, R_c are the mean radii of either graphite or cementite cells and N_g, N_c are the numbers of graphite and cementite eutectic cells per volume or cell densities, and t is the time. Equations (5) and (6) are only valid for f_{ge}/f_{ce} = constant. After solidification, $f_g + f_c = 1$, this in turn indicates that the exponential components in equations (5) and (6) tend to zero. Thus, equations (5) and (6) can be rewritten as:

$$f_g = \frac{f_{ge}}{f_{ge} + f_{ce}} \tag{9}$$

$$f_c = \frac{f_{ce}}{f_{ge} + f_{ce}} \tag{10}$$

In order to estimate the fractions of graphite and cementite eutectics, it is assumed as a first approximation that isothermal conditions prevail for the eutectic transformation (see Fig. 1d), and that the nucleation of eutectic cells is instantaneous, with a constant density ratio N_c/N = const.

Considering the above conditions, Eqs. (7)÷(10) can then be solved using the data from Table 1, and by approximating T_{mst} to T_c in Eq. (8). The calculated fractions, f_g and f_c are schematically shown in Figure 1c. In particular, Figure 1a shows that as the solidification temperature falls below a critical value, T_{cr} the growth rate of cementite eutectic u_c increasingly exceeds the one corresponding to graphite eutectic u_g. Moreover, in the temperature range $\Delta T_{sc} = T_s - T_c$ (where T_c is the formation temperature for cementite eutectic), graphite eutectic is the only growing structure (gray cast iron). Between T_c and T_{cr} (Fig. 1a) both graphite and cementite eutectics are simultaneously developing. However, under these conditions the growth rate of graphite eutectic is dominant. Below T_{cr}, both structures can be still formed, but the growth rate of cementite eutectic is exceedingly large becoming the dominant structure. Below T_w (see Fig. 1a) cementite eutectic is the only constituent formed ($f_c = 1$ for white cast iron, Fig. 1c), while between T_c and T_w mottled cast iron is obtained. Accordingly, T_c can be considered as the transition temperature for the solidification of cementite eutectic from graphite eutectic, or the chill formation temperature. This temperature[1)] is influenced by the cast iron chemistry, and it can be determined from the equation given in Table 1.

[1)] Influence of cooling rate on temperature T_c can be neglected; change cooling rate from 1.8 to 45.0°C/s gives changes only $T_c \approx 2$°C.

Table 1. Selected thermophysical data

Parameter and units	Value
Latent heat of graphite eutectic, J/cm^3	L_e = 2028.8
Latent heat of austenite, J/cm^3	L_γ = 1904.4
Specific heat of cast iron, J/(cm^3·^{o}C)	c = 5.95
Growth coefficient of graphite eutectic, cm/(^{o}C^2·s)	$\mu_g = 10^{-6}\left(9.2 - 6.3\ \mathrm{Si}^{0.25}\right)$
Growth coefficient of cementite eutectic [9], cm/(^{o}C^2·s)	$\mu_c = 2.5\ 10^{-3}$
Moulding material ability to absorb heat, J/(cm^2·s$^{1/2}$ ^{o}C)	a = 0.10
Liquidus temperature for austenite [29], ^{o}C	T_l = 1636 –113(C + 0.25 Si + 0.5 P)
Graphite eutectic equilibrium temperature [29], ^{o}C	T_s = 1154.0 + 5.25 Si – 14.88 P
Cementite eutectic formation temperature [28], ^{o}C	T_c = 1130.56 + 4.06(C – 3.33 Si – 12.58 P)
$\Delta T_{sc} = T_s - T_c$, ^{o}C	ΔT_{sc} = 23.34 – 4.07C +18.80 Si + 36.29 P
Carbon content in graphite eutectic [29], %	C_e = 4.26 – 0.30 Si – 0.36 P
Maximum carbon content in austenite at T_s [29], %	C_γ = 2.08 – 0.11 Si – 0.35 P
Liquidus temperature of austenite when melt composition is equal to the maximum composition of carbon in austenite, $T_{l\gamma} = T_l(C_\gamma)$, ^{o}C	$T_{l\gamma}$ = 1636 –113(2.08 + 0.15 Si + 0.14 P)
Wedges angle, ^{o}: – for small wedge – for big wedge	 β = 28,5 β = 25
Weight fraction of austenite	$g_\gamma = (C_e - C)/(C_e - C_\gamma)$
Austenite density, g/cm^3	ρ_γ = 7.51
Melt density, g/cm^3	ρ_m = 7.1
Volume fraction of austenite	$f_\gamma = \rho_m g_\gamma / [\rho_\gamma + g_\gamma(\rho_m - \rho_\gamma)]$
C, Si, P – content of carbon, silicon and phosphorus in cast iron, respectively, %	

2. ANALYSIS

The changes associated with heat extraction as they relate to the relative energies of solid and liquid phases can be described in two ways:

1) a reduction in the enthalpy of the liquid or solid due to cooling given by $\Delta H = \int c dT$, where c is the heat capacity of the liquid or solid,
2) a release of the heat of solidification through the enthalpy contribution ΔH, also known as the latent heat L; the heat transfer process can then be described by the heat balance equation

$$q_m = q_s - q_a \tag{11}$$

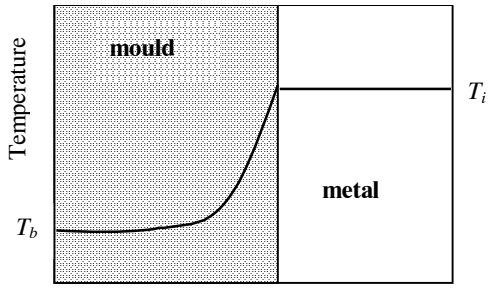

Fig. 2. *Temperature distribution in metal-mould systems*

During the solidification process, the heat transfer events can be rather complex and analytical solutions are not always available, so numerical methods have to be employed. Nevertheless, in sand castings, it can be assumed as the first approximation that heat transfer is mainly determined by the properties of the sand mold [29]. Figure 2 shows the ideal temperature profile expected for sand mold-metal systems. Accordingly, the heat flux density going into the mold can be given by [29]

$$q_m = \frac{T\,k_m}{\sqrt{\pi\,\alpha_d\,t}} \tag{12}$$

Taking into account the thermal diffusivity ($\alpha_d = k_m/c_m$) and the surface area (F_c) of the casting, Eq. (12) can be rearranged as

$$q_m = \frac{a\,F_c T}{\sqrt{\pi\,t}} \tag{13}$$

where $a = \sqrt{k_m c_m}$.

Moreover, it is assumed that the temperature distribution along the metal is uniform (Fig. 2). Hence, the accumulated heat flux in the metal can be given by

$$q_a = \frac{cV_c dT}{dt} \tag{14}$$

The heat flux q_s generated during solidification depends on the specific solidification mechanisms and in general it can be described by

$$q_s = L_e N_g\,V_c\,\frac{dV}{dt} \tag{15}$$

where dV/dt is the volumetric solidification rate of eutectic cells (cm^3/s).

During the analysis of cooling and solidification of cast iron, three stages can be identified (Fig. 3).

In the first stage, the excess heat of molten metal is dissipated and the temperature falls from the initial temperature T_i to the liquidus temperature T_l in the $0 \le t \le t_l$ time interval.

The second stage is characterized by the solidification of the pre-eutectic austenite in the $T_l \leq T \leq T_s$ temperature range and in the $t_l \leq t \leq t_s$ time interval, where t_s is the time at the onset of graphite eutectic solidification.

Finally, the third stage can be attributed to the early stages of solidification of graphite eutectic, which are found to occur between the temperature T_s and the minimum temperature T_m in the $t_s \leq t \leq t_m$ time interval.

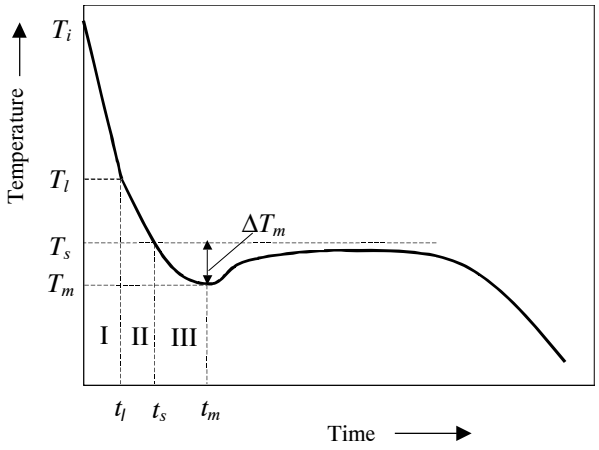

Fig. 3. *Cooling curve for cast iron*

First Stage

During this stage there is no heat generation due to solidification ($q_s = 0$). Accordingly, substitution of equations (13) and (14) into (11), followed by integration for the initial conditions $t = 0$ at $T = T_i$ yields

$$t = \left(AM \ \ln \frac{T_i}{T} \right)^2 \tag{16}$$

where:

$$A = \frac{c\sqrt{\pi}}{2\,a} \tag{17}$$

$$M = \frac{V_c}{F_c} \tag{18}$$

When T equals T_l (temperature at the onset of austenite crystallization), the time $t = t_l$ elapsed during the first cooling stage is given by

$$t_l = (ABM)^2 \tag{19}$$

where

$$B = \ln \frac{T_i}{T_l} \tag{20}$$

Second Stage

The second stage includes the cooling and solidification of pre-eutectic austenite from the liquidus temperature T_l to the beginning of eutectic solidification T_s. It is assumed that the heat generated during the solidification of pre-eutectic phases is uniformly released and the so-called effective specific heat can be used [30].

$$c_{ef} = c + \frac{L_\gamma}{T_{l\gamma} - T_s} \tag{21}$$

At this stage, the temperature of the casting can be estimated from Eqs. (13) and (14) by using c_{ef} instead of c in equation (14)) and then integrating with the limiting conditions $T = T_l$, at $t = t_l$.

This yields

$$t = \left(A_1 M \ \ln \frac{T_l}{T} + \sqrt{t_l} \right)^2 \tag{22}$$

From this expression, the temperature of the metal in the second stage can be described by

$$T = T_l \exp\left(- \frac{\sqrt{t} - \sqrt{t_l}}{A_1 M} \right) \tag{23}$$

Differentiation of the above equation yields an expression for the cooling rate of cast iron

$$\frac{dT}{dt} = - \frac{T_l}{2 A_1 M \sqrt{t}} \exp\left(- \frac{\sqrt{t} - \sqrt{t_l}}{A_1 M} \right) \tag{24}$$

where

$$A_1 = \frac{c_{ef} \sqrt{\pi}}{2\, a} \tag{25}$$

From Eq. (22) after taking into account Eq. (19), the time ($t = t_s$, $T = T_s$) at the end of the second stage can be found as

$$t_s = \left(\frac{M \sqrt{\pi}}{2\, a} \phi \right)^2 \tag{26}$$

The cooling rate at the end of the second stage (or the beginning of third stage) can be established from Eq. (24) for the time ($t = t_s$). Hence, taking into account Eqs. (19) and (26) the cooling rate can be given by[2)]

$$\frac{dT}{dt} = Q = \frac{2\,\mathrm{T_s}\;a^2}{\pi\,\phi\;c_{ef}\;M^2} \tag{27}$$

where

$$\phi = cB + c_{ef}B_1 \tag{28}$$

and

$$B_1 = \ln\frac{T_l}{T_s} \tag{29}$$

Third Stage

During this stage, the portion of the cooling curve (Fig. 2) where the transformation to graphite eutectic occurs can be described in terms of the degree of undercooling ΔT_g as

$$T = T_s - \Delta T_g \tag{30}$$

Although, the degree of undercooling is not explicitly known in the $t_s \geq t \geq t_m$ time range, it can be described by [28]:

$$\Delta T_g = T_s - T = \Delta T_m \sin\left[\omega(t - t_s)\right] \quad \text{for} \quad 0 \leq [\omega(t - t_s)] \leq \pi/2 \tag{31}$$

where $\Delta T_m = T_s - T_m$ (see Fig. 3) is the maximum degree of undercooling, and the frequency ω is given by

$$\omega = \frac{\pi}{2\left(t_m - t_s\right)} \tag{32}$$

Therefore, the cooling rate in the third stage can be found by substitution of Eq. (31) into Eq. (30) followed by differentiation with time. This yields[2)]

$$\frac{dT}{dt} = \Delta T_m \omega \cos\left[\omega\left(t - t_s\right)\right] \tag{33}$$

[2)] It is assumed that cooling rate has a positive sign.

It can be assumed that at the onset of eutectic solidification ($t = t_s$), the cooling rate in stages two and three is the same. Hence, equating Eqs. (27) and (33) yields

$$\frac{dT}{dt} = \omega \, \Delta T_m \tag{34}$$

which after taking into account Eq. (32) can be rewritten as

$$\frac{dT}{dt} = \frac{\pi \Delta T_m}{2(t_m - t_s)} \tag{35}$$

Moreover, using Eqs. (26), (27) and (35), the time for maximum undercooling can be determined from

$$t_m = \frac{\pi \phi M^2 \left(\phi T_s + \pi c_{ef} \Delta T_m \right)}{4 T_s a^2} \tag{36}$$

In addition, at the time t_m, the cooling curve exhibits a minimum, which in turn means that the heat accumulation flux q_a is zero. Considering that the transformed volume of graphite eutectic is $V_c (1 - f_\gamma)$, and Eqs. (13), (15), as well as the condition $q_a = 0$ at $t = t_m$, Eq. (11) becomes

$$\frac{aTF_c}{\sqrt{\pi t_m}} = L_e N_g V_c \left(1 - f_\gamma\right) \frac{dV_m}{dt} \tag{37}$$

also, assuming that in the early stages of growth the eutectic cells are spherical, the volumetric rate of solidification can be described by

$$\frac{dV_m}{dt} = 4\pi R_m^2 \frac{dR_m}{dt} \tag{38}$$

where R_m is the radius of eutectic cells at the maximum degree of undercooling ΔT_m.

Furthermore, the growth rate of eutectic cells is in general described by Eq. (1) as

$$u_g = \frac{dR_g}{dt} = \mu_g \Delta T_g^2 \tag{39}$$

and for $\Delta T_g = \Delta T_m$

$$u_m = \frac{dR_m}{dt} = \mu_g \Delta T_m^2 \tag{40}$$

Substituting Eq. (31) into (39) followed by integration for the initial condition $R = 0$ for $t = t_s$ yields

$$R_g = \frac{\mu_g \Delta T_m^2}{4\omega}\left\{2\omega\left(t - t_s\right) - \sin\left[2\omega\left(t - t_s\right)\right]\right\} \tag{41}$$

At the maximum degree of undercooling ($t = t_m$) and taking into account that $t_m - t_s = \pi/(2\omega)$ from Eq. (32), it is obtained

$$R_g = R_m = \frac{\mu_g \pi \Delta T_m^2}{4\omega} \tag{42}$$

During the eutectic transformation the temperature does not exhibit significant changes and $T \approx T_s$ in Eq. (37). Thus, Eqs. (36) to (38) and Eqs. (40), (42) can be used to arrive at the following expression for the casting modulus

$$M^2 = \frac{8\omega^2 a^2 T_s^{3/2}}{\pi^4 N_g L_e \varphi^{1/2}\ \mu_g^3\ \Delta T_m^6\ \left(1 - f_\gamma\right)\left(\pi\, c_{ef} \Delta T_m + \varphi T_s\right)^{1/2}} \tag{43}$$

It can be assumed that the cooling rate at the end of the second stage is the same as the cooling rate at the beginning of the third stage. Accordingly, a comparison between Eqs. (27) and (34) yields

$$\omega = \frac{2a^2 T_s}{\pi\ \phi\ c_{ef} \Delta T_m M^2} \tag{44}$$

Substituting Eq. (44) into (43) yields

$$M = \frac{2^{5/6} a}{\pi}\left[\frac{T_s^{7/2}}{N_g (1 - f_\gamma) L_e c_{ef}^2 \mu_g^3 \varphi^{5/2} \Delta T_m^8 \left(\varphi T_s + \pi\, c_{ef} \Delta T_m\right)^{1/2}}\right]^{1/6} \tag{45}$$

where

$$\Delta T_m = T_s - T_m \tag{46}$$

In the above expression, the ($\pi\, c_{ef} \Delta T_m$) term in the denominator does not have a significant effect on the equation predictions and can be neglected. Thus, Eq. (45) becomes

$$M = p\left[\frac{1}{N_g \left(1 - f_\gamma\right) \mu_g^3 \Delta T_m^8}\right]^{1/6} \tag{47}$$

where $p = \dfrac{2^{5/6} a T_s^{1/2}}{\pi \phi^{1/2} c_{ef}^{1/3} L_e^{1/6}}$ (48)

Also, after taking into account Eq. (27)

$$p = MQ^{1/2} \frac{2^{1/3} c_e^{1/3}}{\pi^{1/2} L_e^{1/6}} \tag{49}$$

3. CHILLING TENDENCY AND CHILL OF CAST IRON

During solidification nucleation of cells is heterogeneous in nature. A simple model for heterogeneous nucleation has already been proposed [18]. Because every nucleus of graphite give origin to one single graphite eutectic cell, the density of graphite eutectic cells, N_g can be described by [19]

$$N_g = N_s \exp\left(-\frac{b}{\Delta T_m}\right) \tag{50}$$

where $b = \dfrac{4\, T_s \sigma \sin\theta}{L_e \langle l \rangle}$ (51)

In Eq. (50), N_s is the density of substrates available for the nucleation of graphite, σ is the interfacial energy between the graphite nucleus and the melt, θ is the wetting angle between substrate and graphite nucleus, L_e is the latent heat of graphite eutectic, $\langle l \rangle$ is the mean nucleation site size.

Combining equations (47) and (50) leads to the expression

$$M = p \left[\frac{1}{N_s \left(1 - f_\gamma\right) \mu_g^3 \ \Delta T_m^8} \exp\left(\frac{b}{\Delta T_m}\right) \right]^{1/6} \tag{52}$$

or

$$\Delta T_m = T_s - T_m = \frac{b}{8\ \mathrm{ProductLog}[y]} \tag{53}$$

where

$$y = \frac{b\, M^{3/4} \left[N_s \ \left(1 - f_\gamma\right) \mu_g^3 \ \right]^{1/8}}{8\, p^{3/4}} \tag{54}$$

The ProductLog[y] = x is the Lambert function[3], also is called the omega function, which is used to solve equation of the type of $y = xe^x$ (see Fig. 4). ProductLog[y] is non-elementary function which is known as the Lambert – function and also is called the omega function. Its exact values can be easily calculated using the instruction of the ProductLog[y] in the Mathematica™ programme. In our analysis typical values of variable y are situated within ranges of 0.03–500, and in case if we cannot use Mathematica programme its value can be calculated by means of elementary mathematics with an accuracy higher than 99% using the following equations:

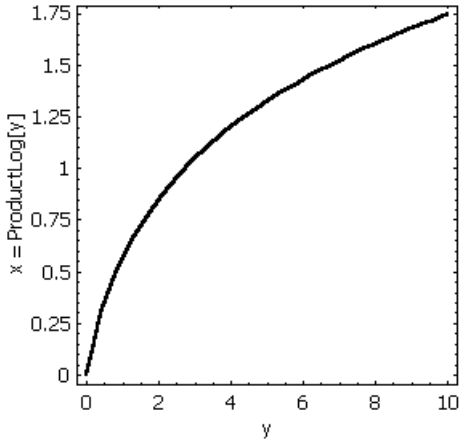

Fig. 4. *Graphic representation of the function ProductLog[y] for $y \geq 0$*

– for $0.03 \leq y \leq 1$ range

$$x = \frac{0.232541y}{-0.03066y^2 + 0.204476y + 0.235837} \tag{55}$$

– for $1 \leq y \leq 5$ range

$$x = \log(0.0855561)y^{0.224539} + 3.03131y^{0.294488} \tag{56}$$

– for $5 \leq y \leq 20$ range

$$x = \log(0.06014)y^{0.00796} + 3.29565y^{0.135821} \tag{57}$$

– for $20 \leq y \leq 50$ range

$$x = \log(0.038806)y^{-0.04997} + 3.59672y^{0.110107} \tag{58}$$

– for $20 \leq y \leq 500$

$$x = \log(0.059427)y^{-0.34418} + 2.03579y^{0.144835} \tag{59}$$

---

[3] See http://mathworld.wolfram.com./LambertW-function.html.

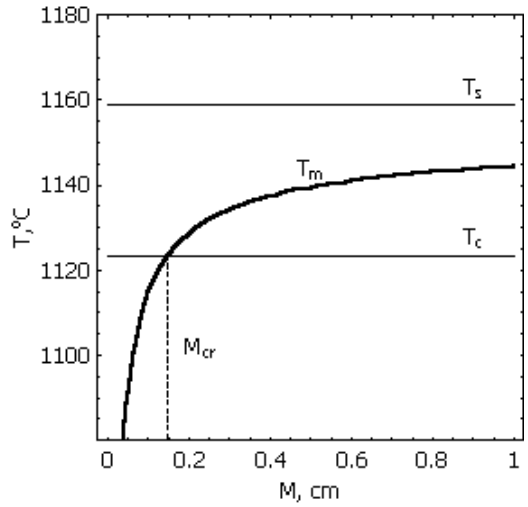

Fig. 5. *Effect of the casting modulus on the minimal solidification temperature T_m for graphite eutectic based on the calculation data: C = 3.5%, Si = 1.2%, P = 0.1%, Ti = 1250°C, b = 100°C, $N_s = 6 \cdot 10^6$ cm^{-3}, rest of data see Table 1*

Equation (53) is graphically plotted in Figure 5. From this figure, it is apparent that the minimum temperature for the solidification of graphite eutectic T_m depends on M, and for values above M_{cr} it falls in between T_s and T_c. Hence, the critical ΔT_m value can be given by $T_s - T_c = \Delta T_{sc}$. Since at temperatures below T_c, the solidification of cementite eutectic becomes dominant, the critical casting modulus M_{cr} under which it is possible to develop a chill can be obtained from Eq. (52) as

$$M_{cr} = p \ \mathrm{CT} \tag{60}$$

where CT is the chilling tendency of cast iron

$$\mathrm{CT} = \left[\frac{1}{N_s \left(1 - f_\gamma\right) \mu_g^3 \ \Delta T_{sc}^8} \exp\left(\frac{b}{\Delta T_{sc}} \right) \right]^{1/6} \tag{61}$$

Similarly, from Eq. (47) the expression for the chilling tendency can be simplified as

$$\mathrm{CT} = \left[\frac{1}{N_t \left(1 - f_\gamma\right) \mu_g^3 \ \Delta T_{sc}^8} \right]^{1/6} \tag{62}$$

where N_t is the cell count at $T = T_c$

Typical values for the chilling tendency range from 0.4 $s^{1/2}/^{o}C^{1/3}$ (inoculated cast iron) to 1.5 $s^{1/2}/^{o}C^{1/3}$(non-inoculated cast iron). Figure 6 shows the influence of the chilling tendency of cast iron on the critical casting modulus. Notice that as the chilling tendency increases, M_{cr} also increases. In establishing the chilling tendency, it is common to implement a set of chilling tests on castings, which consist of cylindrical pins of various diameters *d*. Alternatively, plates with different wall thickness *s* are also employed.

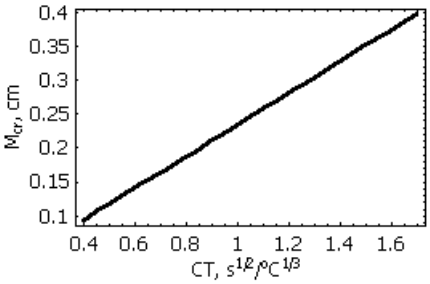

Fig. 6. *Effect of the chilling tendency CE on the critical casting modulus M_{cr} based on the data used for Figure 3*

For these geometries the casting modulus yield:

– for pins of diameter *d* and *a* length that easily exceeds *d*, $M = V_c / F_c = (\pi\, d^2 / 4)/(\pi\, d)$; hence, the critical pin diameter below which the chill is expected to form is given by

$$d_{cr} = 4M_{cr} \tag{63}$$

– for plates with wall thick nesses *s* and lengths and widths which easily exceed *s*, $M = V_c/F_c = (sF_c)/(2F_c)$, and the critical wall thickness below which the chill forms is given by

$$s_{cr} = 2M_{cr} \tag{64}$$

In the foundry practice an assessment of the chilling tendency of cast iron is based on the chill test methods established by the ASTM A367-55T standard. In this case, wedge geometries are employed (Fig. 7). As a first approximation, assuming that the wedge length is rather large, the critical casting modulus M_{cr} can be estimated by

$$M_{cr} = \frac{F_{ch}}{m} = \frac{\frac{1}{2} h \frac{w}{2}}{\frac{h}{\cos(\beta/2)}} \tag{65}$$

and the wedge value is given by

$$w = \frac{4M_{cr}}{\cos(\beta/2)} \tag{66}$$

In the above expressions, β is the wedge angle, F_{ch} is the half surface area chill triangle, *h* and *m* are chill height and length (Fig. 7). The wedge is not a planar body such as the plate.

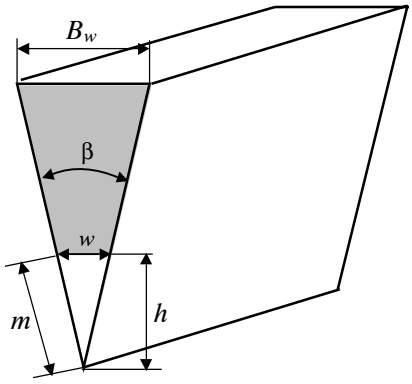

Fig. 7. *Graphic description of the geometry for wedge shaped castings*

Accordingly, the wedge thinner parts heat up from the thicker sections, and the wedge value for wedges of constant chilling tendency depend on their sizes (wedge number according to the ASTM A 367-55T standard). The influence of the wedge size on the wedge value can be found by combining Eqs. (60) and (66). Accordingly, the wedge width of the chill can be expressed as a function of the wedge size coefficient n as

$$w = \frac{4np}{\cos(\beta/2)}\ \mathrm{CT} \tag{67}$$

From the theoretical perspective, the role of the various factors involved on the chilling tendency can be disclosed based on Eq. (62) as:

– The graphite eutectic growth coefficient μ_g, depends on the cast iron chemistry. However, with the exception of silicon, little is known about the influence of other elements on μ_g. Reported values for μ_g are given for Fe-C, Fe-C-0.1% Si [8], and Fe-C-2% Si [26] systems. In general, Si lowers the eutectic growth coefficient (see Fig. 8), and the μ_g dependency on Si can be described by

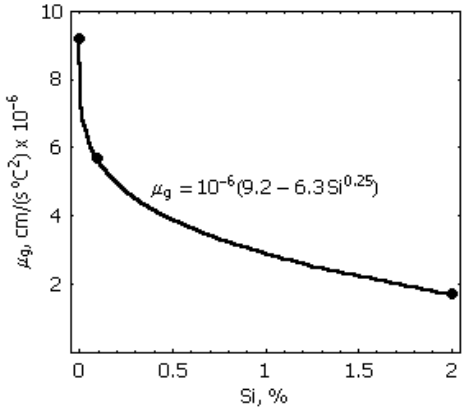

Fig. 8. *Influence of silicon on the graphite eutectic growth coefficient μ_g, experimental points from [8] and [26]*

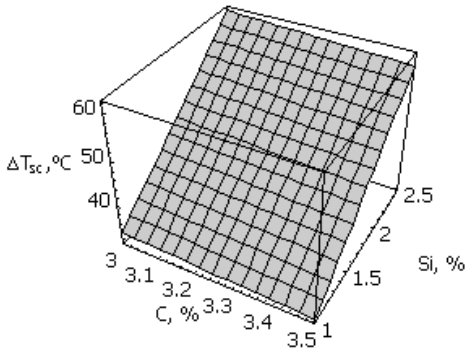

Fig. 9. *Influence of carbon and silicon content on the ΔT_{sc} range*

$$\mu_g = 10^{-6}\left(9.2 - 6.3\ \mathrm{Si}^{0.25}\right)\ \ \mathrm{cm/(s\cdot\ ^oC^2)} \tag{68}$$

so as Si content increases the chilling tendency of cast iron (see Eqs. (18), (19)) also increases.

– The temperature range $\Delta T_{sc} = T_s - T_c$, also depends on the melt chemistry as (see Tab. 1)

$$\Delta T_{sc} = 23.34 - 4.07\ \mathrm{C} + 18.80\ \mathrm{Si} + 36.29\ \mathrm{P}\quad {}^{o}\mathrm{C} \tag{69}$$

where C, Si, and P are the carbon, silicon and phosphorus contents in the cast iron in wt. % From the above expression, it can be observed that silicon and phosphorus expand the ΔT_{sc} range, while C has the opposite effect. Yet, the influence of carbon is relatively small as observed in Figure 9. In turn, this suggests that as Si and P contents increase, the ΔT_{sc} range also increases, and from Eqs. (61), (62) the chilling tendency for cast iron decreases.

– The effect of the volumetric fraction of austenite f_γ, can be described by

$$f_\gamma = \frac{\rho_m \; g_\gamma}{\rho_\gamma + g_\gamma(\rho_m - \rho_\gamma)} \tag{70}$$

where:

$$g_\gamma = \frac{C_e - C}{C_e - C_\gamma} \tag{71}$$

$$C_e = 4.26 - 0.30\ \mathrm{Si} - 0.36\ \mathrm{P} \tag{72}$$

$$C_\gamma = 2.08 - 0.11\ \mathrm{Si} - 0.35\ \mathrm{P} \tag{73}$$

g_γ – mass fraction of austenite,

ρ_γ and ρ_m – the density of austenite and the melt (see Tab. 1),

C_e and C_γ – the carbon content in the graphite eutectic and in the austenite at temperature T_s.

In this case, the influence of phosphorus on the resultant austenite fraction is negligible. Therefore, increasing the amount of carbon and silicon (Fig. 10) lowers the volume fraction of austenite, thus reducing the chilling tendency (Eqs. (61) and (62)).

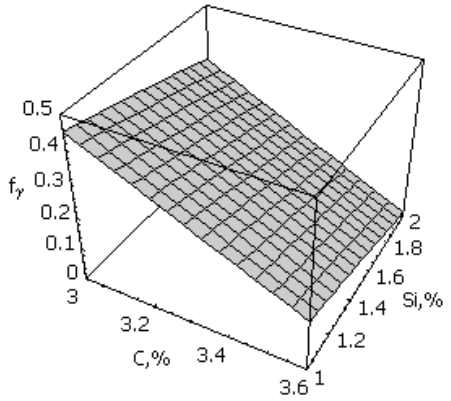

Fig. 10. *Influence of carbon and silicon content on the austenite fraction f_γ in cast iron (P = 0.1%)*

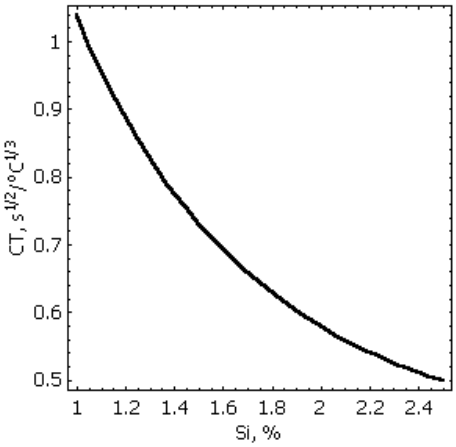

Fig. 11. *Influence of silicon content on the chilling tendency based on the data used for Figure 3*

– Nucleation effects. Depending on the graphite nucleation tendency, in cast iron at a given cooling rate (for example at a given wall thickness) various densities of graphite eutectic cells can be developed. The nucleation tendency for graphite cells is characterized by N_s and the b coefficient, where b is a function of the surface energy, wetting angle and substrate mean size, as shown in Eq. (51). These coefficients generally depend on the melt chemistry, but a detailed account of the influence of alloying elements on these coefficients is not available. Estimations made for the influence of silicon on the chilling tendency (Eqs. (61), (68)–(73)), assuming that b and N_s are constant are graphically illustrated in Figure 11. In general, notice from this figure that Si lowers the chilling tendency of cast iron in agreement with the foundry practice.

Other effects such as the mean graphite nucleation sites sizes $\langle l \rangle$ and total number of sites N_s (Eqs. (50) and (51)), continually change during the bath holding times leading

to mutual interactions. Among the potential interactions are chemical reactions (which also depend on furnace slag and atmosphere), coagulation, coalescence, flotation, etc. Consequently, $\langle l \rangle$ and N_s, both tend to decrease with an increase in the bath holding times (Figs. 12a and 12c) [18]. In addition, increasing bath holding times lead to an increase in the b coefficient as shown in Figure 12b, and to an increase in the chilling tendency (Eq. (61) and Fig. 12d). Moreover, it is well known that the inoculation treatment increases the cell density N by up to one order of magnitude when compared with the base cast iron, thus decreasing the chilling tendency (Eq. (62)).

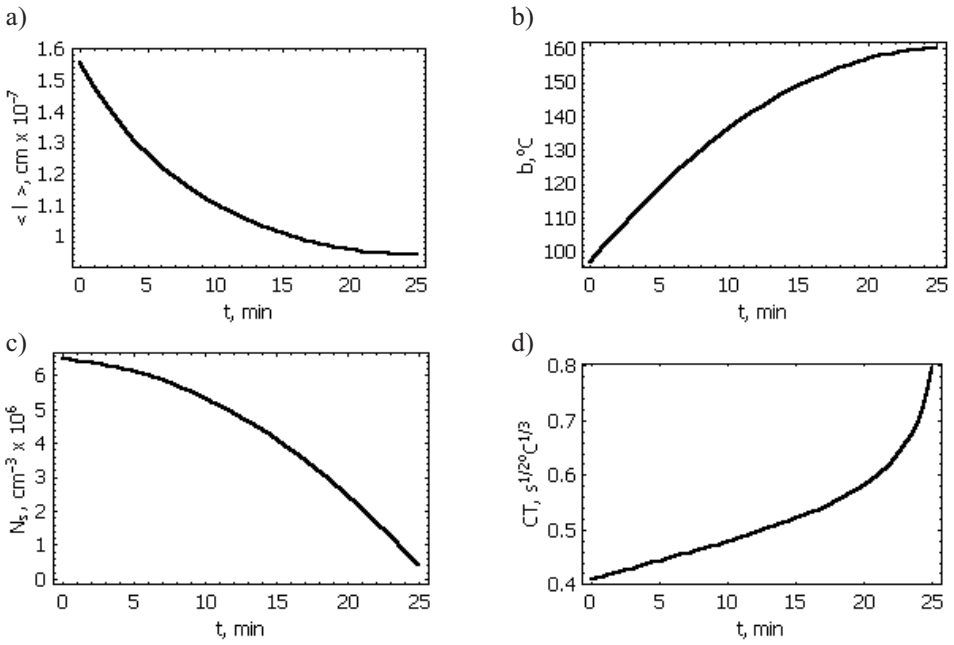

Fig. 12. *Influence of bath holding time on: a) mean substrate size; b) nucleation coefficient; b, c) mean substrate density (N_s) [18]; d) chilling tendency (C = 3.16%, Si = 2.08%, P = 0.091 %, Ti =1250°C)*

From the aforementioned arguments, the chilling tendency CT and in consequence the wedge value of cast iron strongly depends on:

- chemical composition of the casting (through f_g, μ_g, ΔT_{sc}, N_s, and b),
- inoculation practice, first and foremost (through N_s and b),
- superheating temperature and holding time of bath (through N_s and b),
- furnace slag end atmosphere (through N_s and b).

A schematic representation of the influence of the technological factors, which affect the chilling tendency and chill of cast iron are given in Figure 13. It is worth mentioning that the theoretical predictions of this work are in good agreement with the available data published in the literature. In particular, it is well known that the chill of cast iron decreases

with increasing eutectic cell density [20]. Also, the density of graphite eutectic cells N is strongly affected by the melt chemistry [20, 21], superheating bath temperature and time [2] and furnace slag and atmosphere [22]. In practice a drastic increase in the density of cells is usually attained by the use of inoculants. In this case, the resultant cell density depends on the type of inoculant [23–25], quantity [20, 22, 24], granulation [20], inoculation temperature [20], and bath holding times after inoculation [19, 20].

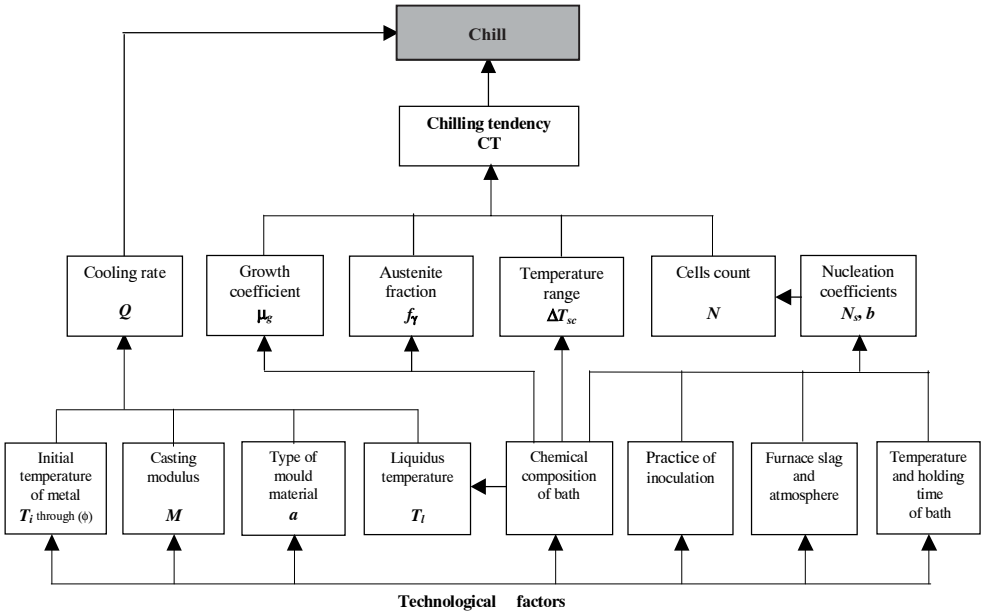

Fig. 13. *Schematic representation of the effect of various technological factors on the chilling tendency of cast iron*

4. CONCLUSIONS

In this work, a simple theoretical treatment is presented for the transition from gray to white cast irons. The proposed analysis is based on a heat balance during solidification. The analysis incorporates the nucleation of eutectic cells, as well as growth effects associated with the eutectic and pre-eutectic phases. From the proposed theory, an expression is derived to relate the chilling tendency of cast iron with the casting modulus. This in turn, enables the determination of minimum wall thickness for chilled castings, or wedge values in wedge shaped castings. Finally, the present work gives a description of the effects of various factors of technological importance on the chill and chilling tendency of cast iron.

This work was supported by Statutory Grant No. 11.11.170.250 and made in Department of Cast Iron AGH-UST, Cracow, Poland.

REFERENCES

[1] *Boyes J.W., Fuller A.G.*: Chill and Mottle formation in cast iron. BCIRA Journal, 12 (1964), 424

[2] *Fuller A.G.*: Effect of superheating on chill and mottle formation. BCIRA Journal, 9 (1961), 693

[3] *Dawson J.V., Maitra S.*: Recent research on the inoculation of cast iron. British Foundrymen, 4 (1957), 117

[4] *Kubick E.J., Javaid A., Bradley F.J.*: Investigation on Effect C, Si, Mn, S and P on Solidification Characteristics and Chill Tendency of Gray Iron – Part II: Chill Tendency. AFS Transaction 103 (1997), 579

[5] *Oldfield W.*: The chill-reducing mechanism of silicon in cast iron. BCIRA Journal, 10 (1962), 17

[6] *Girshovitz N*: Solidification and properties of cast iron. Masinostroyene, Moscow-Leningrad, 1966 (in Russian)

[7] *Magnin P., Kurz W.*: Competitive Growth of Stable and Metastable Fe-C-X Eutectics: Part II. Mechanisms. Metallurgical Transactions, 19A (1988), 1965

[8] *Magnin P., Kurz W.*: Transition from grey to white and to grey in Fe-C-X eutectic alloys. In: The physical metallurgy of cast iron, Fredrickson H., Hillert M. (Eds), North Holland, New York, 1985, 263

[9] *Nastac L., Stefanescu D.M.*: Prediction of grey-to-white transition in cast iron by solidification modelling. AFS Transaction, 103 (1995), 329

[10] *Stefanescu D.M.*: Science and Engineering of Casting Solidification, Kulwer Academic/Plenum Publishers, New York, 2002

[11] *Nastac L., Stefanescu D.M.*: Modelling of stable-to-metastable structural transition in cast iron. In: Physical Metallurgy of Cast Iron V, Lesoult G., Lacaze J. (Eds), Scitec Publications, Switzerland, 1997, 469

[12] *Magnin P. Kurz W.*: An analytical model of irregular eutectic growth and its application to Fe-C. Acta Metallurgica, 35 (1987), 1119

[13] *Hillert M.*: Some theoretical considerations in nucleation and growth during solidification of graphite and white cast irons. In: Recent Research on Cast Iron, Gordon and Breach, Science Publishers, Merchant H. (ed.), New York, 1968, 101

[14] *Tiller W.A.*: Isothermal solidification of Fe-C and Fe-C-Si alloys. in: Recent Research on Cast Iron, Gordon and Breach, Science Publishers, Merchant H. (Ed.), New York, 1968, 129

[15] *Hillert M., Subba Rao V.V.*: Grey and white solidification of cast iron. The Solidification of Metals. The Institute of Metals, London, 1968, No. 110, 204

[16] *Kołmogorov.*: Izwiestija AN SSSR, USSR – Ser. Matemat., 3 (1937), 355

[17] *Kasuya T., Ichikawa K., Bhadeshia D.H.*: Real and extended volumes in simulation transformations. Materials Science and Technology, 15 (1999), 471

[18] *Fraś E., Wiencek K., Górny M., Lopez H.*: Nucleation and grain density – a theoretical model and experimental verification. Archives of Metallurgy, 46 (2001), 317

[19] *Fraś E., Górny M., Tartera J.*: Nucleation and grain density – a theoretical model and experimental verification. International Journal of Cast Research, 16 (2003), 99

[20] *Merchant H.D.*: Solidification of Cast Iron. In: Recent Research on Cast Iron, Gordon and Breach, Merchant H. (Eds), Science Publishers, New York, 1968, 1÷100.

[21] *Oldfield W.*: The solidification of hypo-eutectic grey cast iron. BCIRA Journal, 8 (1960), 177

[22] *Fraś E., Lopez H., Podrzucki C.*: The influence of oxygen on the inoculation process of cast iron. International Journal of Cast Metals Research, 13 (2000), 107

[23] *Fraś E., Podrzucki C.*: Inoculated cast iron. AGH Editor, Cracow, 1982, No. 675 (in Polish)

[24] *Fraś E., Serano T., Bustos A.*: Fundiciones de Hierro. ILAFA, Chile, 1990

[25] *Elliott E.*: Cast Iron Technology. Butterworths, London, 1988

[26] *Lux B., Kurz W.*: Solidification of Metals. The Iron and Steel Institute, London, 1967, 193

[27] *Kubick E.J., Javaid A., Bradley F.J.*: Investigation of effect of C, Si, Mn, S and P on solidification characteristic and chill tendency of gray iron–Part I: Thermal Analysis Results, AFS. Transactions, 105 (1997), 573

[28] *Fraś E., Lopez H.*: A theoretical analysis of the chilling susceptibility of hypoeutectic Fe-C alloys, Acta Metallurgica and Materialia, 41 (1993) 12, 3575

[29] *Chvorinov N.*: Theorie der Erstarrung von Gusstucken. Die Giesserei, (1940) 27, 10

[30] *Longa W.*: General theoretical background of the differential analysis of the casting cooling curves. Archives of Metallurgy, 28 (1983), 281

Received
January 2005